Atmospheric Environment 264 (2021) 118713

Contents lists available at ScienceDirect

Atmospheric Environment

journal homepage: www.elsevier.com/locate/atmosenv

Impacts of the COVID-19 economic slowdown on ozone pollution in the U. S.

Patrick C. Campbell [a,b,*], Daniel Tong [a,b,c], Youhua Tang [a,b,c], Barry Baker [a,b], Pius Lee [b], Rick Saylor [b], Ariel Stein [b], Siqi Ma [c], Lok Lamsal [d], Zhen Qu [e]

[a] Center for Spatial Information Science and Systems, Cooperative Institute for Satellite Earth System Studies, George Mason University, Fairfax, VA, USA
[b] Office of Oceanic and Atmospheric Research, Air Resources Laboratory, National Oceanic and Atmospheric Administration, College Park, MD, USA
[c] Department of Atmospheric, Oceanic and Earth Sciences, George Mason University, Fairfax, VA, USA
[d] Universities Space Research Association, NASA Goddard Space Flight Center, Greenbelt, MD, USA
[e] Harvard University, Department of Engineering and Applied Science, Cambridge, MA, USA

HIGHLIGHTS

- Observations and chemical transport modeling are used to quantify COVID-19 lockdown impacts on ozone pollution in the U.S.
- Widespread emissions decreases lead to widespread ozone decreases in rural regions, but local increases in urban regions.
- There is considerable spatiotemporal variability for the 2020 ozone changes compared to the previous five years.

ARTICLE INFO

Keywords:
COVID-19 economic slowdown
Ozone pollution in the U.S.
CMAQ Model
National Air Quality Forecast Capability

ABSTRACT

In this work, we use observations and experimental emissions in a version of NOAA's National Air Quality Forecasting Capability to show that the COVID-19 economic slowdown led to disproportionate impacts on near-surface ozone concentrations across the contiguous U.S. (CONUS). The data-fusion methodology used here includes both U.S. EPA Air Quality System ground and the NASA Aura satellite Ozone Monitoring Instrument (OMI) NO_2 observations to infer the representative emissions changes due to the COVID-19 economic slowdown in the U.S. Results show that there were widespread decreases in anthropogenic (e.g., NO_x) emissions in the U.S. during March–June 2020, which led to widespread decreases in ozone concentrations in the rural regions that are NO_x-limited, but also some localized increases near urban centers that are VOC-limited. Later in June–September, there were smaller decreases, and potentially some relative increases in NO_x emissions for many areas of the U.S. (e.g., south-southeast) that led to more extensive increases in ozone concentrations that are partly in agreement with observations. The widespread NO_x emissions changes also alters the O_3 photochemical formation regimes, most notably the NO_x emissions decreases in March–April, which can enhance (mitigate) the NO_x-limited (VOC-limited) regimes in different regions of CONUS. The average of all AirNow hourly O_3 changes for 2020–2019 range from about +1 to −4 ppb during March–September, and are associated with predominantly urban monitoring sites that demonstrate considerable spatiotemporal variability for the 2020 ozone changes compared to the previous five years individually (2015–2019). The simulated maximum values of the average O_3 changes for March–September range from about +8 to −4 ppb (or +40 to −10%). Results of this work have implications for the use of widespread controls of anthropogenic emissions, particularly those from mobile sources, used to curb ozone pollution under the current meteorological and climate conditions in the U.S.

* Corresponding author. Center for Spatial Information Science and Systems, Cooperative Institute for Satellite Earth System Studies, George Mason University, Fairfax, VA, USA.

E-mail address: patrick.c.campbell@noaa.gov (P.C. Campbell).

https://doi.org/10.1016/j.atmosenv.2021.118713
Received 22 January 2021; Received in revised form 2 August 2021; Accepted 2 September 2021
Available online 4 September 2021

1. Introduction

The global confinement due to rising COVID-19 cases, in particular, travel restrictions and quarantining shelter-in-place orders are associated with significant decreases in surface transportation activity by about 50% globally (Le Quéré et al., 2020). Consequently, the COVID-19 economic slowdown led to a "natural air pollution control experiment" due to widespread anthropogenic emissions reductions for atmospheric pollutants and their precursor gases, such as decreased oxides of nitrogen ($NO_x = NO + NO_2$) emissions of up to ~ 50% (Zhang et al., 2020; EEA, 2020; U.S. EIA, 2020). The COVID-19 impacts on air pollution occurred on a scale impossible to reproduce outside of such a global health emergency.

The emission reductions during the lockdown measures led to varying changes in air quality conditions across the world. During February–March 2020 in China, surface fine particulate matter ($PM_{2.5}$) and carbon monoxide (CO) concentrations decreased by about 25% and 17%, respectively (Yue et al., 2020). It was approximated that although air pollutant emissions decreased by 40% in the Northern China Plain, there were high levels of $PM_{2.5}$ (hourly levels >200 μg m^{-3}) that persisted from late January to mid-February, while surface ozone (O_3) also increased sharply by 84% (Li et al., 2020). In other cities, there were substantial decreases in NO_x (56%) and $PM_{2.5}$ (42% in Wuhan and 8% in Europe), but surface ozone (O_3) increased in all cities (36% in Wuhan and 17% in China) (Sicard et al., 2020). In fact, analyses of COVID-19 related air pollution changes show that ground level O_3 increased by 2–30% for 11 cities globally (Shi et al., 2021). Ground-level O_3 is formed by chemical reactions of volatile organic compounds (VOCs) and NO_x in the presence of sunlight, and its production rate can be altered via different chemical regimes and environments around the world (Sillman et al., 1990; Sillman 1995, 1999; Pusede et al., 2012; Jin et al., 2013; Walaszek et al., 2018; Li et al., 2019). High O_3 concentrations can lead to decreased lung function and cause impaired respiratory symptoms, which are particularly dangerous for young children, the elderly, and those with preexisting conditions including asthma, chronic obstructive pulmonary disease (COPD), lung cancer, and respiratory infection (Kar Kurt et al., 2016).

The COVID-19 economic slowdown and related traffic decreases that reached up to ~50% during March–May in the U.S. (INRIX; U.S. News, 2020) led to notable changes in pollutants in urban areas of the country, particularly for NO_2 concentrations that declined significantly as recorded from both satellite- and ground-based observations. Ground-based monitors indicated statistically significant declines for NO_2 of 26.0% or 5.4 ppb in urban counties (Berman et al., 2020), while the TROPOspheric Monitoring Instrument (TROPOMI) satellite observations showed that the NO_2 decreases ranged between 9.2% and 43.4% among 20 cities in North America (Goldberg et al., 2020). Qu et al. (2021) finds that surface and satellite NO_2 measurements at U.S. EPA ground based sites with the 5% highest concentrations show consistent reductions of 22–26% in March–April and 8–13% in May–June 2020 compared to the same months in 2019.

It was clear by mid-May in the U.S, however, that surface O_3 levels had not fallen in coincidence with decreasing NO_x levels across much of the U.S. (NPR, 2020), where various analyses showed variable O_3 changes across different U.S. regions (Arunachalam et al., 2020; Ivey et al., 2020; Kang et al., 2020; Van Haasen, 2020; Yang et al., 2020). The high spatial O_3 variability may have been exacerbated by relaxed shelter-in-place orders for many U.S. states in early-to mid-June that led to rebounding anthropogenic emissions in some regions.

Motivated by the apparent COVID-19 related O_3 variability in different global regions and in portions of the U.S., we hypothesize that there are regional differences in the impact of COVID-19 lockdowns on O_3 formation across the U.S. This study combines the use of both ground and satellite-based observations of NO_2 to infer changes in precursor emissions due to the COVID-19 economic slowdown, and then uses the derived emission changes and a chemical transport model to quantify the related changes in O_3 concentrations across the entire contiguous U.S. (CONUS). Here we focus on O_3 as an indicator of pollution changes due to the COVID-19 economic slowdown in the U.S. because 1) changes in traffic NO_x emissions strongly impact O_3 formation, 2) O_3 is the dominating pollutant contributing to non-attainment zones in the warm summer months (Zhang et al., 2019; U.S. EPA, 2020), and 3) because O_3 has well-defined health impacts (Anenberg et al., 2009; Fann et al., 2012).

2. Methodology

2.1. Model configuration and observations

The National Air Quality Forecasting Capability (NAQFC) used in this work is a well-documented and evaluated air quality modeling system (Eder et al., 2006, 2009; Mathur et al., 2008; Stajner et al., 2011; Lee et al., 2017). The NAQFC used in this work is based on the offline-coupled North American Mesoscale Model Forecast System on the B-Grid (NMMB) (Black, 1994; Janjic and Gall, 2012), which provides the driving weather data to the Community Multiscale Air Quality (CMAQ) model, version 5.0.2 (U.S. EPA, 2012). CMAQ simulates the formation, transport, and fate for a suite of atmospheric composition parameters. The NAQFC has provided real-time air quality forecast guidance over the past decade for different EPA-defined criteria pollutants, including near-surface O_3 at a horizontal resolution of 12 × 12 km centered over CONUS. The main chemical configurations for the NAQFC includes the CB05-TuCl/Aero6 gas-aerosol phase mechanism with simple aqueous phase chemistry reactions (see Lee et al., 2017 for further details). The NAQFC chemical initial conditions are started from a "warm-start" off of previous operational model output ending on March 01, 2020 and incur a two-week spin-up time (i.e., March 01–14 is removed from analyses). The time-dependent chemical lateral boundary conditions below 7 km altitude are provided by the Goddard Earth Observing System-Chemistry (GEOS-Chem; http://acmg.seas.harvard.edu/geos/) model output for 2006 that are mapped to appropriate CMAQ species and tuned for the operational NAQFC (Bey et al., 2001; Lam and Fu, 2009; Tang et al., 2009). We note that the version of the NAQFC used here has some slight differences compared to the operational NAQFC products (i.e., BASE simulation: see Section 2.2 below), which includes use of a single cycle 12Z forecast (as opposed to 4-cycle 00, 06, 12, and 18Z runs), and omission of wildfire emissions. These NAQFC configuration differences are not expected to make appreciable impacts on the O_3 changes under the COVID-19 scenarios investigated here.

The U.S. EPA AirNow observation network data (https://www.airnow.gov/) are ideally suited for studying the ongoing impacts of the COVID-19 economic slowdown on O_3 as they provide real-time air quality information across the U.S. for over 2,000 monitoring stations via the AirNow Application Programming Interface (https://docs.airnowapi.org/), while also maintaining a consistent historical data record and format to readily compare the average conditions of air pollution for different U.S. regions. The AirNow observation data are downloaded, processed/analyzed, and paired in space and time with the NAQFC simulation grid cells for the same hourly time periods using NOAA's Model and Observation Evaluation Toolkit (MONET) (Baker and Pan, 2017). The AirNow observations are used to assess the spatial changes in O_3 and to compare and evaluate the NAQFC simulations.

2.2. Emissions adjustment methodology and simulation design

The NAQFC 2020 simulations are based on the U.S. EPA National Emissions Inventory 2014v2 (NEI2014v2; U.S. EPA, 2018), and form the "BASE" case. We quantify the COVID-19 effect using the difference between a "business-as-usual" (BAU) and COVID-19 (C19) case, both based on the NEI2014v2 emissions (the BASE case). The BASE case is not projected into the forecast year, with the time lag being a long-recognized issue in NAQFC (e.g., Tong et al., 2012). In both BAU and C19 cases, however, the emissions are projected from the BASE year (2014) to 2020. BAU and C19 use the same observation-based trend adjustment for the period of 2014–2019, with the only difference being the change from 2019 to 2020.

In the BAU case, the 2019 to 2020 emissions (mobile and area sectors) change is assumed the same as the 2014–2019 period, so the one-year change is the mean changing rate (% per year) from the pre-COVID-19 period. This is the best estimate if the COVID-19 pandemic did not happen. In the C19 case, the observed satellite and ground-based observed NO_2 changing rate from 2019 to 2020 is used to represent the actual emission progression under the pandemic. Compared to the annual emission changes in the pre-COVID-19 period, there was a much larger change from 2019 to 2020 in many states of the CONUS.

For both cases, we derive the NO_2 trend data using the approach developed by Tong et al. (2015, 2016). In this approach, the emission-changing rate for each state is derived according to the following equation:

$$AF=\frac{\Delta S\times N_s\times f_s+\Delta G\times N_G\times f_G}{N_s\times f_s+N_G\times f_G} \tag{1}$$

where AF is the emission adjustment factor (rate of emission change), ΔS and N_S are the rate of change and the number of satellite data, respectively. ΔG and N_G are the rate of change and the number of ground-based data, respectively. f_S and f_G are two weighting factors applied to the satellite and ground data, respectively. The values of ΔS and ΔG are calculated for each state using the vertical column density from the Ozone Monitoring Instrument (OMI) aboard the Aura satellite (Levelt et al., 2006, 2018), and the U.S. EPA Air Quality System (AQS) ground network (https://www.epa.gov/aqs), respectively. Here the value of f_S is set to be 1 and f_G to be 100 to place more weight in the ground-based AQS observations, and the OMI data is filtered with a low-value cutoff value (0.7×10^{15}) to further remove influence from retrieval noise and background sources of NO_2 (Tong et al., 2015, 2016). Furthermore, the AQS NO_2 changes are selected from the early morning rush hours (0600, 0700, and 0800 local time) that are more representative of transportation emission sector changes during the COVID-19 economic slowdown (Tong et al., 2016). Further details on the data processing and quality control procedures are provided in Tong et al. (2015). We use OMI as opposed to other newer satellite observations (e.g., TROPOMI) because of the well validated, and relatively long data record of OMI dating back to 2004 (Lamsal et al., 2020), which can more appropriately predict the emission trends used in deriving the BAU and COVID-19 cases.

The percent change in emission AFs between March–September (monthly averages) indicate widespread decreases in C19 emissions for March–May, with more states shifting to lesser decreases, or some relative increases by June–September (Fig. 1). The emission AFs are applied to all mobile and area source sectors and emission species, which impact their associated chemical species and consequential O_3 formation in the NAQFC simulations under each scenario. The difference in the predicted O_3 concentrations between the BAU and C19 cases is attributed to the impact of the pandemic. Emissions from point/energy generating units are not adjusted in this study. The full simulation period analyzed in this study is March 01 – September 30, 2020 and is focused on the CONUS region.

3. Results

3.1. Changes in anthropogenic emissions

The COVID-19 related economic slowdown generally led to decreased NO_x emissions, but there is also state-to-state variability (Fig. 2).

Between March–June (Fig. 2a–c), many states in the east (e.g., New York) showed a relatively large decrease in NO_x emissions (up to ~ 50–65%; Supporting Fig. S1), while states in the west experienced smaller decreases (<25%) and some increases (e.g., Montana and South Dakota). During May–June (Fig. 2c and d) and the following months, states in the east show progressively smaller emission decreases, with some states shifting to relative emission increases compared to BAU. Interestingly, some states in the west show larger emission decreases during and after June.

The calculated emission trends in the Central and Eastern U.S. mainly indicate lower NO_x emissions for C19 compared to BAU for March–April, which then predominantly increase over time and become more similar to the BAU emissions by June–July. In fact, the C19 NO_x emissions become higher than BAU for the Southeast and Upper Midwest U.S. in July (Fig. 3).

The regional and state-level variability in BAU and C19 emissions changes are impacted by differences in state-mandated shelter-in-place and partial recovery activities that occurred later in the spring and summer months during the pandemic, and largely from the impact that these protocols had on emissions from on-road passenger vehicles across the U.S. Mobility data from Apple Inc. (Apple Inc., 2020) indicates that there were widespread driving decreases and relatively high variability in March–May, which shifts to general driving increases and lower spatial variability in May–September (Supporting Fig. S2). This does not fully account for different transportation modes, and excludes much of the national and state-level truck traffic used in large-scale domestic shipping (i.e., Federal Highway Administration vehicle classes 5–13 or vehicle length >23 feet), which did not show similar trends (https://www.ms2soft.com/traffic-dashboard/).

Relative to passenger vehicle emissions, the emissions from commercial vehicles and electricity demand sources are relatively unchanged and impacts the changes in secondary air pollution formation during the COVID-19 lockdown (Archer et al., 2020). This affects the use of OMI-AQS NO_2 changes that are inclusive of all emission sector changes during COVID-19. Other emissions studies also agree with the timing of emissions changes estimated here and indicate that there were 13% decreases in transportation-related emissions early in March–May 2020 (Shilling et al., 2020), and then rebounding emission trends from May–July, particularly by mid-June through September when states

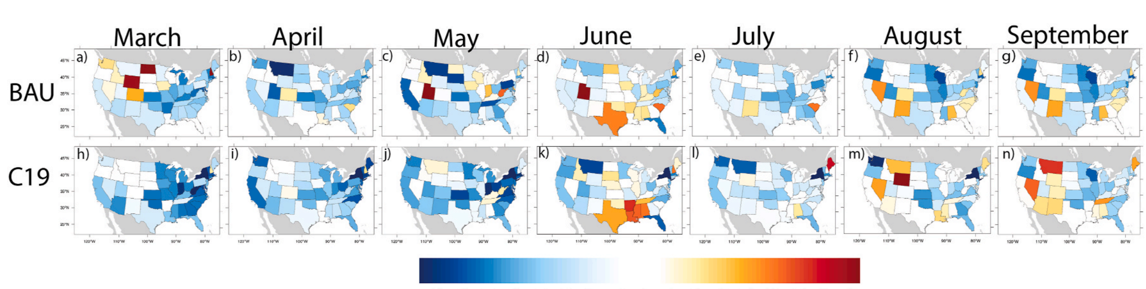

Fig. 1. Percent changes in monthly average emission adjustment factors (AFs) (based on Eq. (1)) for the a)-g) "Business-As-Usual" (BAU) and h)-n) COVID-19 (C19) cases.

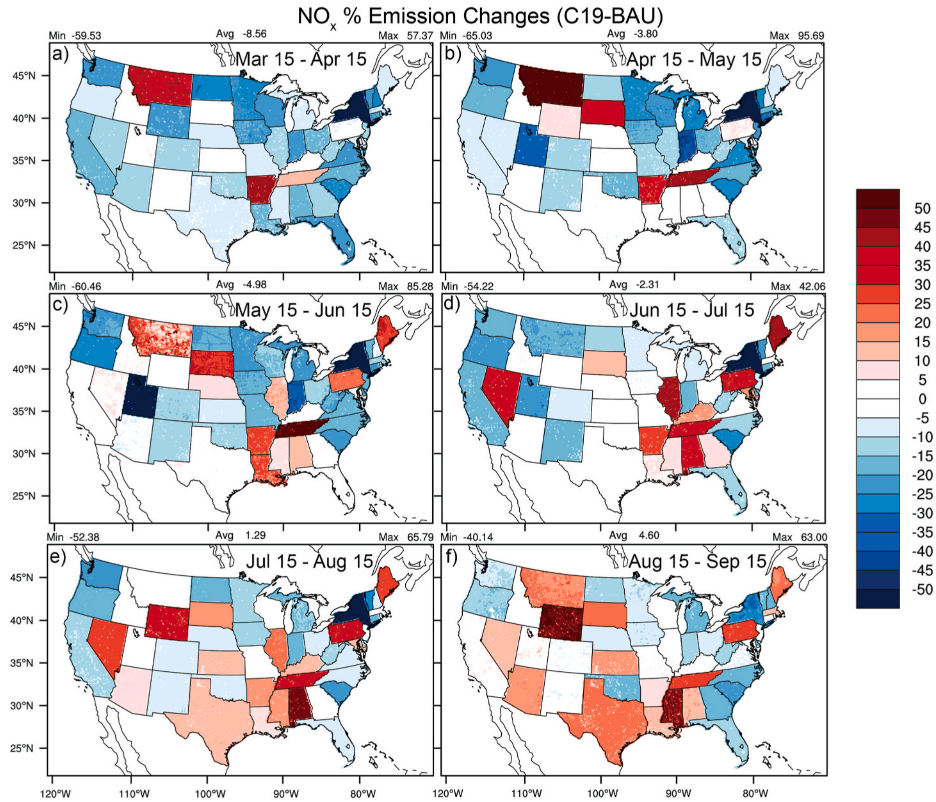

Fig. 2. Average percent changes for NO_x emissions ([C19-BAU/BAU]*100%) between a) March 15 – April 15, b) April 15 – May 15, c) May 15 – June 15, d) June 15 – July 15, e) July 15 – August 15, and f) August 15 – September 15. The associated absolute changes in NO_x emissions are found in Supporting Fig. S1.

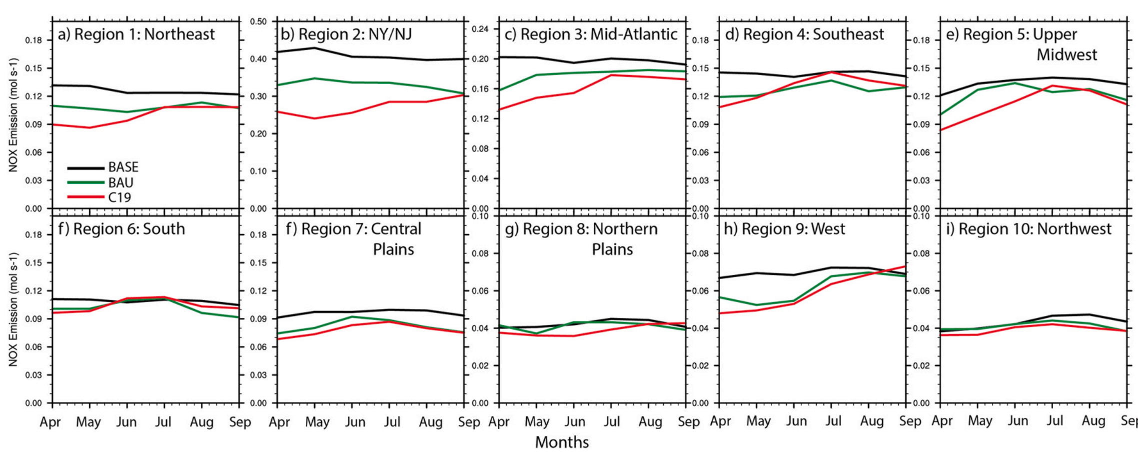

Fig. 3. Regional NO_x emissions (mol s^{-1}) trends ending on April 15 – September 15, 2020 for the BASE (black; NEI2014v2), "Business-As-Usual (BAU) (green), and COVID-19 (C19) (red) cases in the different U.S. EPA regions (https://www.epa.gov/aboutepa/regional-and-geographic-offices). Note the change in emissions scales on the y-axis. (For interpretation of the references to colour in this figure legend, the reader is referred to the Web version of this article.)

began lifting restrictions (Le Quéré et al., 2020). Furthermore, the shift to cleaner vehicle fleets in the BAU trend may also have led to fewer emissions compared to the C19 shift to more domestic, heavy-duty truck traffic (typically using diesel fuel) during the morning rush hours compared to less passenger traffic during the lockdown.

The shift to smaller decreases or increases for the OMI-AQS inferred NO_x emissions in the summer months may also be impacted by an increasing background NO_2 concentration that partly limits the use of OMI observations in this work (discussed more below). The western U. S., which is characterized by relatively lower NO_x emissions, indicates smaller decreases for C19 compared to BAU during all months, except September where C19 becomes slightly higher than BAU.

3.2. Comparisons of observed and modeled ozone concentrations

Evaluation of the BASE O_3 simulations (using NEI2014v2 emissions) against the U.S. EPA AirNow network for April–September 2020 shows that the NAQFC model performance is acceptable, while consistently falling within statistical criteria ranges for O_3 in Emery et al. (2017). The exceptions are a slightly high normalized mean bias (NMB) and low correlation coefficient (R) in the Northeast (Supporting Table S1a), and slightly high NMB in the Upper Midwest in May (Table S1e), Central Plains U.S. regions in May, and Northwest U.S. in April–May (Table S1j). The O_3 simulations for the BAU and C19 scenarios demonstrate mainly increases in the correlation, R, and Index of Agreement (IOA), and decreases in Normalized Mean Error (NME) compared to the BASE case.

Analysis of the 2020–2019 changes in observed and simulated BASE maximum daily 8-h average (MDA8) O_3 at 25 of the highly polluted cities for O_3 based on the American Lung Association "State of the Air® 2019" report (American Lung Association, 2020) provides important spatial information on the impacts of the lockdown on local air quality in areas of already elevated pollution (Fig. 4). A similar analysis for the 2020 changes against the previous 5-year average (2015–2019) are shown in Supporting Fig. S3, and are in good agreement with the changes shown in Fig. 4 for 2020–2019.

During the initial COVID-19 lockdown period in March–April, there are predominantly MDA8 O_3 decreases at all sites, with changes ranging from +10% to −35% (e.g., Houston, TX) at the highly polluted cities. Rather expectedly, the BASE simulation does not show as large of an O_3 decrease in March–April due to the use of NEI2014v2 emissions that do not take into account COVID-19 related changes. Later in May and the O_3-season months of June–August in the U.S., there are many more polluted cities that experience MDA8 O_3 increases, particularly in southern California (e.g., El Centro, CA) and eastward (with changes up to ~ +40 to +55%). There is also more observed site-to-site variability during the summer ozone season months in the U.S. The BASE simulation again does not capture the higher variability in ozone changes during the summer months of June–August. Later in September, mainly all sites in California show increases in MDA8 O_3, while all sites in the Mid-Atlantic and the northeast U.S. show decreases. This is in better agreement with the BASE simulations and suggests both rebounding mobile emissions and a potentially strong role from natural, i.e., meteorological variability impacts on the ozone changes.

Overall, the MDA8 O_3 increases are mainly <30%, except for Houston TX in May and August, El Centro CA in July, and Los Angeles and Redding CA in September, which have increases >40%. In the eastern Mid-Atlantic U.S. cities, such as in Arlington, VA, there were relatively small decreases in MDA8 O_3 from March–August (≤15%), but in September there was a larger decrease of ~35%. In the northeast cities, including Hartford, CT, there are moderate MDA8 O_3 changes on the order of about ±15%. The largest decrease (increase) in MDA8 O_3 based on these cities was ~35% (55%) observed at Dallas TX (Houston TX) in March (August), and demonstrate the significant *spatiotemporal* variability in ozone changes during the COVID-19 economic slowdown.

The evaluation results (Supporting Table S1a) and differences in AirNow site comparisons (Fig. 4) against the BASE simulation confirm the importance in projecting the emissions using available observations and the BAU and C19 trend scenarios to quantify the spatial changes in O_3 across the CONUS.

3.3. *Quantifying the COVID-19 related changes in ozone concentrations*

3.3.1. *Observed ozone changes*

Analysis of the observed changes for 2020–2019 shows that there are widespread, moderate decreases in the MDA8 O_3 (Fig. 5a; average ~ −5.8 ppb) and hourly O_3 (Fig. S4a; average ~ −4.3 ppb) across the AirNow sites in March–April, which shifts to smaller decreases and more widespread increases at the sites later in April–May.

Later in May–September there are more variability in the regional changes, where aside from the predominant ozone decreases at the sites in the southeast, there are many regions that show increases such as the upper Midwest and North Central Plains, and much of the western U.S. including California in August–September.

Comparing the observed AirNow ozone conditions between 2020 and 2019 are somewhat limited by the year-to-year variability regardless of the pandemic, and can underestimate the true impact of the COVID-19 economic slowdown. Thus, Table 1 shows the average AirNow hourly and MDA8 O_3 changes for 2020 compared to each individual year during 2015–2019 and the 5-year average. Supporting Figs. S4 and S5 further show spatial difference plots for other previous years (2015–2018) to demonstrate the year-to-year variability.

There are predominantly decreases in hourly and MDA8 observed O_3 for 2020 compared to all previous 5 years, where the largest decreases

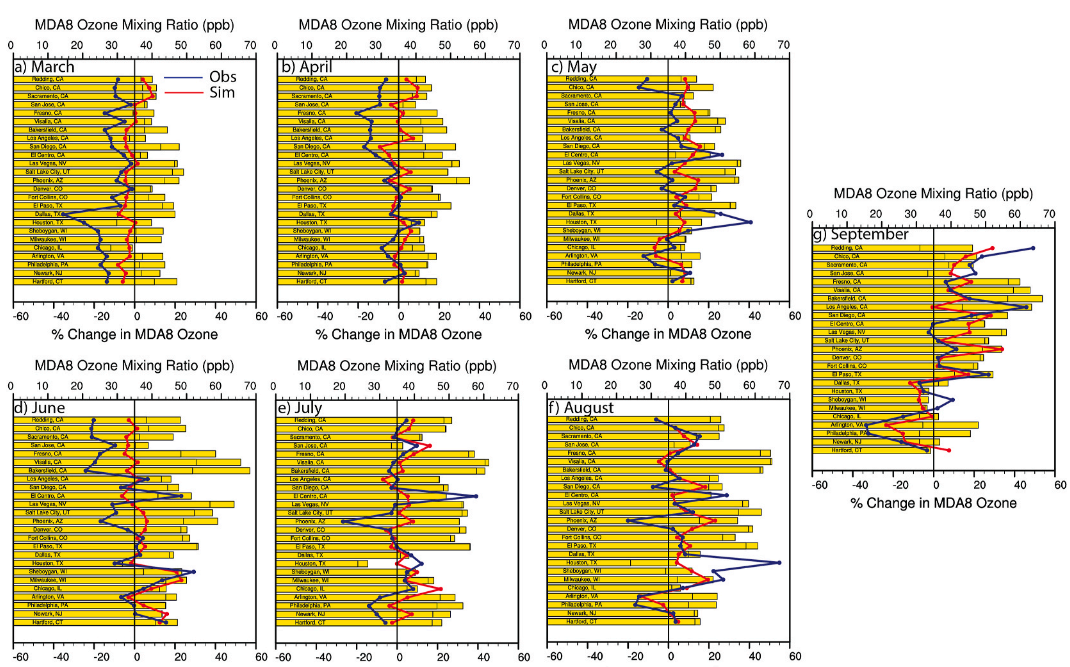

Fig. 4. Horizontal stacked bar chart for observed 2019 and 2020 monthly average median MDA8 O_3 mixing ratio (top-axis) and corresponding percent change ({[2020–2019]/2019}*100%) in AirNow observed (bottom axis; navy blue line/symbols) and simulated BASE (i.e., operational NAQFC with NEI2014v2 emissions) MDA8 O_3 (bottom axis; red line/symbols) at 25 specific AirNow observation sites (labeled in bar charts) based on highly ozone polluted cities in the American Lung Association "State of the Air® 2019" report for a) March, b) April, c) May, d) June, e) July, f) August, and g) September. If the % change is positive, the stacked bar chart's first/bottom line is 2019 and the second/top line is 2020. If the % change is negative, the first/bottom line is 2020 and second/top line is 2019. (For interpretation of the references to colour in this figure legend, the reader is referred to the Web version of this article.)

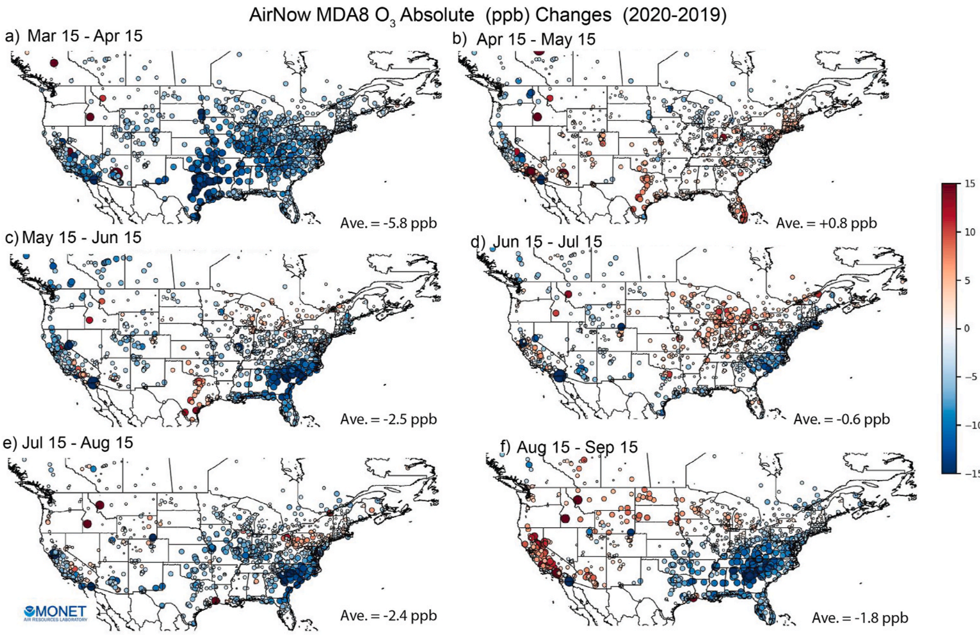

Fig. 5. Average absolute changes (2020–2019) for observed AirNow MDA8 O_3 (ppb) between a) March 15 – April 15, b) April 15 – May 15, c) May 15 – June 15, d) June 15 – July 15, e) July 15 – August 15, and f) August 15 – September 15. Average of all sites are shown in lower right corner of each panel. Supporting Fig. S4a shows the similar 2020–2019 spatial changes for hourly O_3.

Table 1
Average of all AirNow site hourly (MDA8) O_3 changes in ppb for the 2020 COVID-19 economic slowdown periods compared to the previous five years (2015–2019).

Period	2020–2019	2020–2018	2020–2017	2020–2016	2020–2015	Average
Mar 15-Apr 15	−4.3 (−5.8)	−3.8 (−4.4)	−3.4 (−4.7)	−1.9 (−2.6)	−1.1 (−2.2)	**−2.9 (-3.9)**
Apr 15-May 15	+1.1 (+0.8)	−3.0 (−4.2)	+0.3 (−0.3)	+0.4 (−0.7)	−0.4 (−2.0)	**−0.3 (-1.3)**
May 15-Jun 15	−1.9 (−2.5)	−1.5 (−2.9)	−2.3 (−3.4)	−2.4 (−4.0)	−1.5 (−2.2)	**−1.9 (-3.0)**
Jun 15-Jul 15	−0.6 (−0.6)	−1.6 (−2.0)	−0.7 (−0.7)	−2.1 (−2.5)	+0.2 (+0.4)	**−1.0 (-1.1)**
Jul 15-Aug 15	−1.6 (−2.4)	−2.4 (−3.7)	−1.0 (−1.9)	−1.3 (−2.0)	−1.0 (−2.0)	**−1.5 (-2.4)**
Aug 15- Sep 15	−1.4 (−1.8)	−0.6 (−0.4)	−1.7 (−2.3)	−0.5 (−0.7)	−3.0 (−4.6)	**−1.4 (-2.0)**

Increases are shaded in red and decreases are shaded in blue.

occurred during March–April (Table 1; 5-yr average hourly/MDA8 O_3 ~ −3 ppb/-4 ppb). There are, however, year-to-year variability for the 2020 O_3 changes that demonstrates the role of non-linear formation from varying emissions and meteorological conditions. There are only a few instances of increased 2020 ozone, mostly during April–May, which demonstrated the smallest 5-year average AirNow observed decreases (~−0.3 ppb/-1.3 ppb). There are predominantly decreases in hourly (MDA8) O_3 during June–September that ranged from −1 to −1.5 ppb (−1.1 to −2.4 ppb) for 2020 compared to the 5-year average. The majority of AirNow sites are situated in highly populated, urban/city locations, and are not as representative of the surrounding rural regions in CONUS. Overall, the AirNow observed 2020 O_3 changes in Figs. 4 and 5 show significant spatiotemporal variability during the pandemic period of March–September compared to the previous 5 years (2015–2019), and thus the experimental NAQFC C19 and BAU simulations are further used to quantify the O_3 changes in both urban and rural areas throughout CONUS.

3.3.2. Simulated ozone changes

The differences in the NAQFC sensitivity simulations (C19-BAU) qualitatively agree with AirNow observations and show widespread decreases in monthly average absolute (Fig. 6) and percent O_3 changes (Fig. S6) due to the COVID-19-related mobility changes and reduced NO_x emissions in March–June, which are strongly controlled by the NO_x-limited photochemistry across the rural regions of the U.S.

The robust photochemical indicator O_3/NO_y (Sillman et al., 1997; Liang et al., 2006; Zhang et al., 2009; Campbell et al., 2015) is used here to show the regions of NO_x-limited and VOC-limited chemistry for the BAU and C19 cases in the U.S. (Supporting Figures S8a-S8b). In the major urban regions, there are increases in surface O_3 associated with the NO_x emission decreases. There are also local enhancements in the ozone decreases near urban regions in states with increased NO_x emissions. These regions are characterized by VOC-limited photochemistry, where the decreases (increases) in NO_x emissions lead to increases (decreases) in O_3 formation, as the change in NO_x emissions are in proportion to the change in VOC emissions (not shown). During June–September, there is a shift to more widespread, but relatively smaller increases in O_3 from the south and southeast to western parts of the U.S., which are associated with increases in NO_x emissions across the rural, NO_x-limited regions (Fig. 2), but not near the major urban centers that the model suggests are VOC-limited during this time. The areas of decreased C19 NO_x emissions (more prolific in March–June) tend to enhance the NO_x-limited conditions in the rural areas, and strongly mitigates the VOC-limited conditions in urban areas due to the additional increases in O_3. The areas of increased C19 NO_x emissions (more prolific in June–September) tends to mitigate NO_x-limited conditions near the rural regions, and moderately enhances the already VOC-limited regions in urban regions (Supporting Fig. S8c). We note that uncertainties in the biogenic VOC emissions in the NAQFC simulations will affect the calculation of possible summertime shifts in more NO_x-limited regimes in some locations, particularly in the southeast CONUS where there is significant vegetation.

These results are also in qualitative agreement with the AirNow observations that show more areas of increased O_3 during the summer

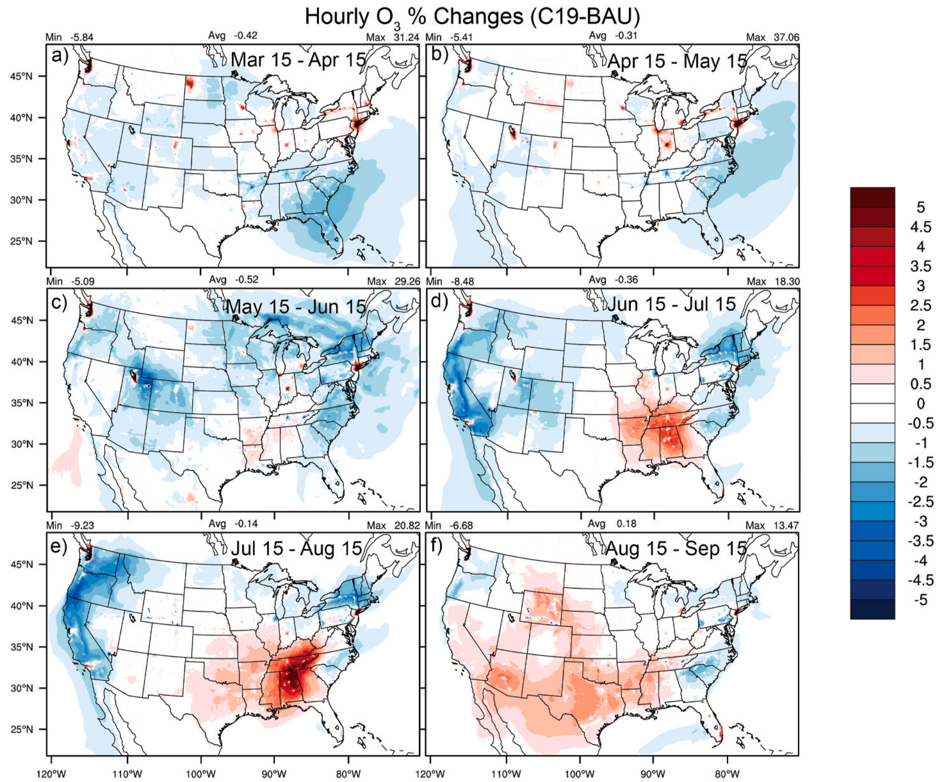

Fig. 6. Average absolute changes for simulated hourly O_3 (ppb) between a) March 15 – April 15, b) April 15 – May 15, c) May 15 – June 15, d) June 15 – July 15, e) July 15 – August 15, and f) August 15 – September 15.

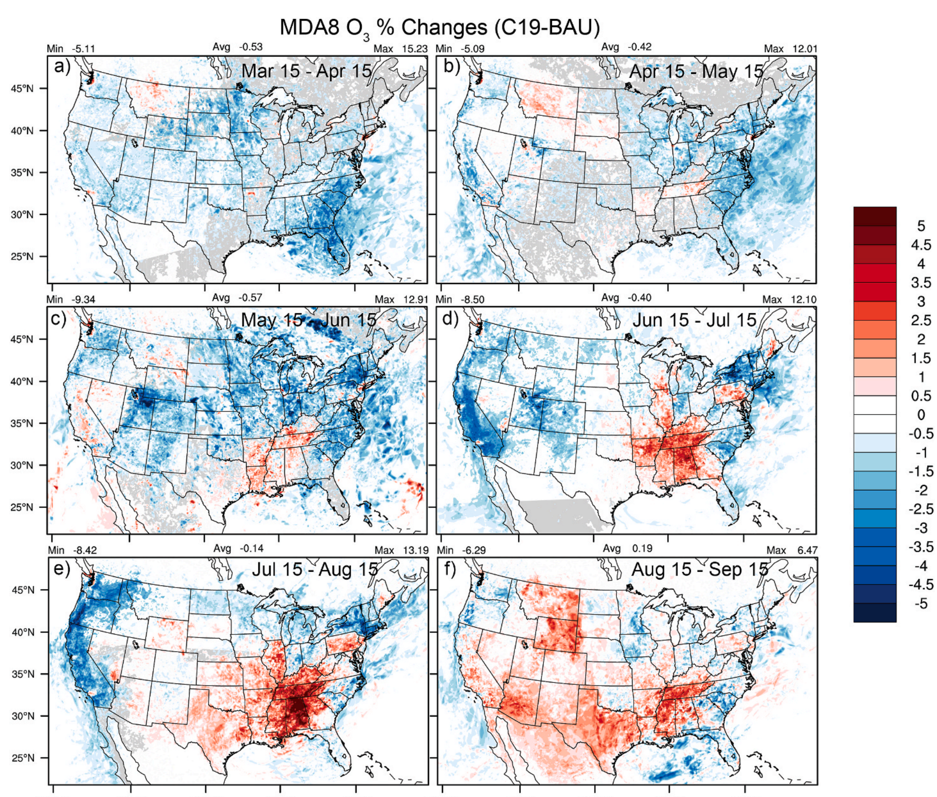

Fig. 7. Same as in Fig. 6, but for the median value of MDA8 O_3.

months, particularly in the central and southern U.S. during June–August, and in California during August–September. The model agreement in the different CONUS regions tends to have dependence on the specific previous year compared to 2020 AirNow observations, where the simulated widespread enhanced ozone increases during summer has arguably the best spatial agreement with the observed 2020–2016 and 2020–2015 changes (Supporting Fig. 4d and e). The simulated shift to more widespread increases in O_3 across the southern U.S. also agrees with NASA's global atmospheric composition model (GEOS-CF) simulations of O_3 that used sustained reductions in global anthropogenic emissions of NO_x, carbon monoxide (CO) and VOCs compared to a BAU scenario. This demonstrates the high non-linearity of O_3 chemistry, which leads to widespread O_3 increases in the southern portions of the U.S. in July–August (Keller et al., 2020). There are also localized increases in simulated ozone during all months in the urban coastline regions of the Long Island Sound (LIS) that span across the New York, New Jersey, and Connecticut state borders. This is in good agreement with the AirNow observations, where there are either hourly ozone increases or weaker decreases in the LIS region for the previous years compared to 2020 (Supporting Figs. S4a-4e).

The spatial patterns for the monthly median absolute (Fig. 7) and percent MDA8 O_3 changes (Supporting Fig. S7) are similar to hourly O_3, but there are indications of larger decreases and increases for MDA8 O_3 in the enhancement regions.

Increases in the peak of daily O_3 values has consequence for the regions close to or in non-attainment for ozone standards. This is particularly true for the south-southeast states and other localized urban areas of the U.S. where increases in MDA8 O_3 of up to ~3–7 ppb may have affected the total number of O_3 exceedance days during the 2020 summer season.

There are also prominent decreases in MDA8 ozone in the northeast and western U.S., most notably in New York State during May–August, and in California, Oregon, and Washington during June–August. Decreases of up to ~3–5 ppb of MDA8 ozone are also important, and can result in alteration of the atmospheric oxidation capacity that can effectively change the production rate of secondary particles during the warm season (not shown). Co-impacts of O_3 and secondary particulate matter formation changes during the COVID-19 pandemic should be more closely studied in future work.

4. Conclusions

Using both observations and NAQFC modeling (based on CMAQv5.0.2) we show that the COVID-19 lockdown caused variable impacts on anthropogenic emissions and both hourly and maximum daily (MDA8) ozone concentrations across the U.S. There were widespread decreases in NO_x emissions in the U.S. during March–June 2020, which led to widespread decreases in O_3 concentrations in the rural regions that are NO_x-limited, but also localized increases near some of the highly populated urban centers that are VOC-limited. Later in June–September 2020, the data-fused AQS and OMI NO_2 changes suggested that many areas in the U.S. showed relative increases in NO_x emissions for the C19 compared to BAU scenarios, and consequently the simulations suggest widespread increases in O_3 concentrations. The widespread NO_x emissions changes also alters O_3 photochemical formation regimes, most notably the NO_x emissions decreases in March–April, which can enhance (mitigate) the NO_x-limited (VOC-limited) regimes in different regions of CONUS.

The average of all AirNow hourly (MDA8) O_3 changes for 2020–2019 range from about +1 to −4 ppb (+1 to −6 ppb) during March–September, and are associated with predominantly urban monitoring sites that demonstrate considerable spatiotemporal variability for the 2020 ozone changes compared to the previous five years (2015–2019). The simulated maximum values of the average hourly (MDA8) O_3 changes for March–September range from about +8 to −4 ppb (+7 to −5 ppb), which correspond to relative changes that range from about +40 to −10% (+15 to −10%). Overall, the variable spatial patterns in modeled ozone changes are in good agreement with the changes at the predominantly urban-limited AirNow sites; however, there are differences that vary depending on the specific previous year compared to 2020 during the COVID-19 pandemic.

To place our results into context, recent international results also show high spatiotemporal COVID-19 related O_3 changes both globally and regionally. Venter et al. (2020) showed that compared to the previous 3-year period, the COVID-19 lockdown led to marginal increases in observed O_3 of about 4% averaged across 34 countries during lockdown dates up until May 15, but that there were both increases and decreases at specific ground observation sites across the U.S. in January–May. This is in qualitative agreement with our results of spatial variability in the year-to-year changes for ground-site observations (Fig. 5 and S4-S5) and model-based results with both increased and decreased O_3 for different CONUS regions by May 15. Chossiere et al. (2021) found that of the 146 of the 252 regions analyzed showed O_3 decreases in response to the COVID-19 lockdowns, with 45 of those regions being statistically significant. However, they further indicate there was no statistically significant change in O_3 concentrations on average across in the U.S., with a range of −5.6 to 4% (mean ~ 0.8%). The contrasting results of Chossiere et al. with our work may be due to different analysis methods, and because we more closely analyzed model-grid cell (12 × 12 km) resolved MDA8 O_3 changes later in the U.S. ozone season, which showed relatively higher local O_3 changes (~−40 to +10%) due to the COVID-19 lockdown. Bray et al. (2021) showed widespread and rather prolific increases in observed ground level O_3 at AirNow ground-based sites during the peak March–April lockdown period in the U.S. The Bray et al. analysis is only in partial agreement with our results of observed AirNow changes in O_3 concentrations in some U.S. regions and specific year-to-year changes, particularly for the regions of increased O_3 in April–May (Table 1, Fig. 5, and Supporting Figs. S4-S5). Indeed, there are some discrepancies between studies for unknown reasons at this time. Our results here extend the quantitative analysis of COVID-19 driven O_3 impacts further into the warmer "ozone season" months in CONUS (i.e., May–September 2020), which have implications for widespread emission changes during the most prolific ozone non-attainment months in the U.S.

Use of the satellite and ground-based NO_2 observations to reflect the actual COVID-19 related emission changes in 2020 has some limitations. The ground-based changes in NO_2 are heavily weighted towards the predominantly urban site locations, where the meteorological conditions and natural NO_2 emission sources, i.e., natural variability, plays an important role in accurately attributing the observed NO_2 changes to NO_x emissions and consequently the NAQFC simulated O_3 concentration changes. Goldberg et al. (2020) found that the NO_2 was relatively low in 2020 (compared to 2019) based on the meteorological conditions in many regions, particularly the prevailing wind directions that transported predominantly clean air masses to major cities areas such as Miami, FL, and Washington D.C. The numerous natural sources of NO_2 (e.g., lighting, soil, and wildfires) that heavily impact background concentrations further confound the use of OMI NO_2 observations to infer the actual COVID-19 related emissions changes, especially during the summer months (Qu et al., 2021).

The COVID-19 economic slowdown and natural experiment of widespread reductions in precursor emissions in different ozone formation regimes in the U.S. has implications for emission control strategies used to curb elevated pollution near major cities and remaining non-attainment areas in the U.S. The impact of the COVID-19 pandemic sheds further light onto the importance of significantly controlling VOC emissions in and around urban areas, such that widespread controls on NO_x emissions are not efficient at reducing ozone levels in regions that experience similar reductions in VOC emissions. This suggests that VOC emission reductions may need to be even greater than NO_x reductions in VOC-limited cities in the spring/summer.

This work shows that there were widespread reductions in ozone levels during the initial period of COVID-19 lockdown, but there are indications of predominantly increased ozone near major cities and possibly more widespread increases later in the summer. It is these regions of elevated ozone that are of concern for those suffering with preexisting health issues, where the increased exposure to air pollution due to the COVID-19 related emissions changes may exacerbate the human susceptibility, health impacts, and spread of the COVID-19 virus itself (Chakrabarty et al., 2020; Wu et al., 2020). Undoubtedly, more research is needed on the interconnections between air quality, exposure and susceptibility, and public health management during widespread pandemics and the many unintended consequences that follow.

Data availability statement

For emissions adjustment factor preparation, the OMI/Aura satellite data are available at https://aura.gesdisc.eosdis.nasa.gov/data/Aura_OMI_Level2/OMNO2.003/ and the U.S. EPA AQS ground observation data are available at the AQS Application Programming Interface (API) at https://aqs.epa.gov/aqsweb/documents/data_api.html. The U.S. EPA AirNow observations are also available via the AirNow API at https://docs.airnowapi.org/. The National Air Quality Forecasting Capability (NAQFC) code used in this work, which is based on CMAQv5.0.2, is published on Zenodo at http://doi.org/10.5281/zenodo.1079888 and is also available for download on GitHub at https://github.com/USEPA/CMAQ/tree/5.0.2. The raw, gridded emissions and NAQFC simulation output are very large (multiple Terabytes) and are freely available in two different ways: (1) on the local NOAA/NCEP repositories that can be directly transferred via SFTP or SCP in pieces, or manually copied in their entirety and provided via external hard drives, and (2) on a publicly available repository/transfer in pieces or via another high-speed file transfer service such as Globus (https://www.globus.org/datatransfer).

Disclaimer

The scientific results and conclusions, as well as any views or opinions expressed herein, are those of the author(s) and do not necessarily reflect the views of NOAA or the Department of Commerce.

CRediT authorship contribution statement

Patrick C. Campbell: Conceptualization, Methodology, Software, Data curation, Visualization, Investigation, Writing – original draft. **Daniel Tong:** Methodology, Writing – review & editing, Project administration, Funding acquisition. **Youhua Tang:** Software, Data curation. **Barry Baker:** Software, Data curation. **Pius Lee:** Software, Data curation, Supervision, Project administration, Funding acquisition. **Rick Saylor:** Supervision, Project administration, Funding acquisition, Writing – review & editing. **Ariel Stein:** Supervision, Project administration, Funding acquisition. **Siqi Ma:** Data curation. **Lok Lamsal:** Data curation, Writing – review & editing. **Zhen Qu:** Writing – review & editing.

Declaration of competing interest

The authors declare that they have no known competing financial interests or personal relationships that could have appeared to influence the work reported in this paper.

Acknowledgments

This study was co-funded by the National Oceanic and Atmospheric Administration's (NOAA's) Weather Program Office (Grant/Contract Number NA19OAR4590082) and the NASA Health and Air Quality Program (Grant/Contract Number 80NSSC21K0512). Support for this work was also provided by NOAA's Office of Oceanic and Atmospheric Research and the Cooperative Institute for Satellite Earth System Studies (CISESS).

Appendix A. Supplementary data

Supplementary data to this article can be found online at https://doi.org/10.1016/j.atmosenv.2021.118713.

References

American Lung Association, 2019. State of the Air. Report. Available at: http://www.stateoftheair.org/.

Anenberg, S.C., et al., 2009. Intercontinental impacts of ozone pollution on human mortality. Environ. Sci. Technol. 43 https://doi.org/10.1021/es900518z, 6482-6287.

Apple LLC "reportApple COVID-19 Community Mobility Reports". https://covid19.apple.com/mobility/Accessed: August 31, 2020.

Archer, C.L., Cervone, G., Golbazi, M., et al., 2020. Changes in air quality and human mobility in the USA during the COVID-19 pandemic. Bull. Atmos. Sci. Technol. https://doi.org/10.1007/s42865-020-00019-0.

Arunachalam, S., Arter, C., Pandey, G., Buonocore, J., 2020. Impacts of COVID-19 related shutdown on onroad and air transportation emissions-related O3, NO2 and PM2.5 in the U.S. Using sensitivity modeling techniques. In: CMAS Virtual Conference, 2020. October 26-30, 2020.

Atlantic Council, 2020. Can We Compare the COVID-19 and 2008 Crises? [Internet]. May 05 [cited 2020 Jun 01]; Available from: https://www.atlanticcouncil.org/blogs/new-atlanticist/can-we-compare-the-covid-19-and-2008-crises/.

Baker, Barry, Pan, Li, 2017. Overview of the model and observation evaluation Toolkit (MONET) version 1.0 for evaluating atmospheric transport models. Atmosphere 8 (11), 210.

Berman, J.D., Ebisu, K., 2020. Changes in U.S. air pollution during the COVID-19 pandemic. Sci. Total Environ. 739, 139864 https://doi.org/10.1016/j.scitotenv.2020.139864.

Bey, I., Coauthors, 2001. Global modeling of tropospheric chemistry with assimilated meteorology: model description and evaluation. J. Geophys. Res. 106 (23) https://doi.org/10.1029/2001JD000807, 073–23 095.

Black, T., 1994. The new NMC meso-scale Eta Model: description and forecast examples. Weather Forecast. 9 (1994), 265–278.

Bray, C.D., Nahas, A., Battye, W.H., Aneja, V.P., 2021. Impact of lockdown during the COVID-19 outbreak on multi-scale air quality. Atmos. Environ. https://doi.org/10.1016/j.atmosenv.2021.118386.

Campbell, P., Zhang, Y., Yahya, K., Wang, K., Hogrefe, C., Pouliot, G., Knote, C., Hodzic, A., San Jose, R., Perez, J., Guerrero, P.J., Baro, R., Makar, P., 2015. A multi-model assessment for the 2006 and 2010 simulations under the air quality model evaluation international initiative (AQMEII) phase 2 over North America: Part I. Indicators of the sensitivity of O3 and PM2.5 formation regimes. Atmos. Environ. 115, 569–586. https://doi.org/10.1016/j.atmosenv.2014.12.026.

Chakrabarty, R.K., Beeler, P., Liu, P., Goswami, S., Harvey, R.D., Pervez, S., van Donkelaar, A., Martin, R.V., 2020. Ambient PM2.5 Exposure and Rapid Spread of COVID-19 in the United States. *Science of the Total Environment*, 143391. https://doi.org/10.1016/j.scitotenv.2020.143391. Advance online publication.

Chossière, G.P., Xu, H., Dixit, Y., Isaacs, S., Eastham, S.D., Allroggen, F., Speth, R.L., Barrett, S.R.H., 2021. Air pollution impacts of COVID-19-related containment measures, 2021 May Sci. Adv.. https://doi.org/10.1126/sciadv.abe1178. PMID: 34020946; PMCID: PMC8139585.

Eder, B., Kang, D., Mathur, R., Yu, S., Schere, K., 2006. An operational evaluation of the Eta-CMAQ air quality forecast model. Atmos. Environ. 40 (26), 4894–4905. https://doi.org/10.1016/j.atmosenv.2005.12.062.

Eder, B., Kang, D., Mathur, R., Pleim, J., Yu, S., Otte, T., Pouliot, G., 2009. A performance evaluation of the national air quality forecast capability for the summer of 2007. Atmos. Environ. 43 (14), 2312–2320. https://doi.org/10.1016/j.atmosenv.2009.01.03.

Emery, C., Zhen, Liu, Armistead, G., Russell, M., Talat, Odman, Greg, Yarwood, Naresh, Kumar, 2017. Recommendations on statistics and benchmarks to assess photochemical model performance. J. Air Waste Manag. Assoc. 67 (5), 582–598. https://doi.org/10.1080/10962247.2016.1265027.

European Environment Agency, 2020 Apr 04. Air Quality and COVID-19 [cited June 02, 2020]. Available from: https://www.eea.europa.eu/themes/air/air-quality-and-covid19.

Fann, N., Lamson, A.D., Anenberg, S.C., Wesson, K., Risley, D., Hubbell, B.J., 2012. Estimating the national public health burden associated with exposure to ambient PM2.5 and ozone. Risk Anal. 32, 81–95. https://doi.org/10.1111/j.1539-6924.2011.01630.x.

Goldberg, D.L., Anenberg, S.C., Griffin, D., Mclinden, C.A., Lu, Z., Streets, D.G., 2020. Disentangling the impact of the COVID-19 lockdowns on urban NO2 from natural variability. Geophys. Res. Lett. 47 (17) https://doi.org/10.1029/2020gl089269.

Ivey, C.E., Gao, Z., Tanvir, S., Do, K., Yeganeh, A.K., Barth, M., Russel, A., Blanchard, C., Lee, S.-M., 2020. Traffic, precursor emissions, and ozone in the south coast air basin during California's COVID-19 shutdown. In: CMAS Virtual Conference, 2020. October 26-30, 2020.

Janjic, Z.I., Gall, R., 2012. Scientific Documentation of the NCEP Nonhydrostatic Multiscale Model on the B Grid (NMMB). Part 1 Dynamics. NCAR Tech. Note NCAR/

TN-4891STR, 75 pp. [Available online at: https://opensky.ucar.edu/islandora/object/technotes%3A502/datastream/PDF/view.
Jin, L., Loisy, A., Brown, N.J., 2013. Role of meteorological processes in ozone responses to emission controls in California's San Joaquin Valley. J. *Geophys. Res. Atmos*. 118, 8010–8022. https://doi.org/10.1002/jgrd.50559.
Kang, D., Hogrefe, C., Murphy, B., Isakov, V., Mathur, R., Gilliam, R., Pouliot, G., Henderson, B., Sidi, F., Sarwar, G., Spero, T., 2020. Air quality changes under COVID-19 social distancing in the United States: observational analysis and modeling sensitivity study. In: CMAS Virtual Conference, 2020. October 26-30, 2020.
Kar Kurt, O., Zhang, J., Pinkerton, K.E., 2016. Pulmonary health effects of air pollution. Curr. Opin. Pulm. Med. 22 (2), 138–143. https://doi.org/10.1097/MCP.0000000000000248.
Keller, C.A., Evans, M.J., Knowland, K.E., Hasenkopf, C.A., Modekurty, S., Lucchesi, R.A., Oda, T., Franca, B.B., Mandarino, F.C., Díaz Suárez, M.V., Ryan, R.G., Fakes, L.H., Pawson, S., 2020. Global impact of COVID-19 restrictions on the surface concentrations of nitrogen dioxide and ozone. Atmos. Chem. Phys. Discuss. https://doi.org/10.5194/acp-2020-685.
Lam, Y.F., Fu, J.S., 2009. A novel downscaling technique for the linkage of global and regional air quality modeling. Atmos. Chem. Phys. 9, 9169–9185. https://doi.org/10.5194/acp-9-9169-2009.
Lamsal, L.N., Krotkov, N.A., Vasilkov, A., Marchenko, S., Qin, W., Yang, E.-S., Fasnacht, Z., Joiner, J., Choi, S., Haffner, D., Swartz, W.H., Fisher, B., Bucsela, E., 2020. OMI/Aura nitrogen dioxide standard product with improved surface and cloud treatments. Atmos. Meas. Tech. Discuss. https://doi.org/10.5194/amt-2020-200.
Le Quéré, C., Jackson, R.B., Jones, M.W., et al., 2020. Temporary reduction in daily global CO2 emissions during the COVID-19 forced confinement. Nat. Clim. Change. https://doi.org/10.1038/s41558-020-0797-x.
Lee, P., McQueen, J., Stajner, I., Huang, J., Pan, L., Tong, D., et al., 2017. NAQFC developmental forecast guidance for fine particulate matter (PM 2.5). Weather Forecast. 32 (1), 343–360. https://doi.org/10.1175/waf-d-15-0163.1.
Levelt, P.F., van den Oord, G.H.J., Dobber, M.R., Mälkki, A., Visser, H., de Vries, J., Stammes, P., Lundell, J., Saari, H., 2006. The ozone monitoring instrument. IEEE T. Geosci. Remote 44. https://doi.org/10.1109/TGRS.2006.872333, 093–1101.
Levelt, P.F., et al., 2018. The ozone monitoring instrument: overview of 14 years in space. Atmos. Chem. Phys. 18, 5699–5745. https://doi.org/10.5194/acp-18-5699-2018.
Li, K., et al., 2019. Anthropogenic drivers of 2013–2017 trends in summer surface ozone in *China*. Proc. Natl. Acad. Sci. U.S.A. 116, 422–427.
Li, M., Wang, T., Xie, M., Li, S., Zhuang, B., Fu, Q., Zhao, M., Wu, H., Liu, J., Saikawa, E., Liao, K., 2020. Drivers for the poor air quality conditions in North China Plain during the COVID-19 outbreak. Atmos. Environ. https://doi.org/10.1016/j.atmosenv.2020.118103.
Liang, J.-Y., Jackson, B., Kaduwela, A., 2006. Evaluation of the ability of indicator species ratios to determine the sensitivity of ozone to reductions in emissions of volatile organic compounds and oxides of nitrogen in northern California. Atmos. Environ. 40, 5156–5166. https://doi.org/10.1016/j.atmosenv.2006.03.060.
Mathur, R., Yu, S., Kang, D., Schere, K.L., 2008. Assessment of the wintertime performance of developmental particulate matter forecasts with the Eta-Community Multiscale Air Quality modeling system. J. Geophys. Res. 113 (D2), D02303 https://doi.org/10.1029/2007JD008580.
NPR, 2020. Traffic Is Way Down Because of Lockdown, but Air Pollution? Not So Much [cited July 08, 2020]. Available from: https://www.npr.org/sections/health-shots/2020/05/19/854760999/traffic-is-way-down-due-to-lockdowns-but-air-pollution-not-so-much?utm_medium=RSS&utm_campaign=science.
Pusede, S.E., Cohen, R.C., 2012. On the observed response of ozone to NOx and VOC reactivity reductions in San Joaquin Valley California 1995–present. Atmos. Chem. Phys. 12, 8323–8339. https://doi.org/10.5194/acp-12-8323-2012, 2012. www.atmos-chem-phys.net/12/8323/2012/.
Qu, Z., Jacob, D.J., et al., 2021. US COVID-19 Shutdown shows Importance of Background NO2 in Inferring Nitrogen Oxide (NOx) Emissions from Satellite NO_2 Observations. In prep.
Shi, Z., Song, C., Liu, B., Lu, G., Xu, J., Van Vu, T., Elliott, R.J.R., Li, W., Bloss, W.J., Harrison, R.M., 2021. Abrupt but smaller than expected changes in surface air quality attributable to COVID-19 lockdowns. Sci. Adv. 7, eabd6696.
Shilling, F., 2020. Special Report 3: Impact of COVID19 Mitigation on Traffic, Fuel Use and Climate Change. Road Ecology Center. UC Davis. April 30, 2020. Available from: https://roadecology.ucdavis.edu/files/content/projects/COVID_CHIPs_Impacts_updated_430.pdf.
Sicard, P., De Marco, A., Agathokleous, E., Feng, Z., Xu, X., Paoletti, E., Rodriguez, J., Calatayud, V., 2020. Amplified ozone pollution in cities during the COVID-19 lockdown. Sci. Total Environ. 735.
Sillman, S., 1995. The use of NOy, H2O2, and HNO3 as indicators for ozone-NOx-hydrocarbon sensitivity in urban locations. J. Geophys. Res. Atmos. 100, 14175–14188.
Sillman, S., 1999. The relation between ozone, NOx and hydrocarbons in urban and polluted rural environments. Millenial Review series. Atmos. Environ. 33 (12), 1821–1845.
Sillman, S., Logan, J.A., Wofsy, S.C., 1990. The sensitivity of ozone to nitrogen oxides and hydrocarbons in regional ozone episodes. J. Geophys. Res. 95, 1837–1852.
Sillman, S., He, D., Cardelino, C., Imhoff, R.E., 1997. The use of photochemical indicators to evaluate ozone-NOx-hydrocarbon sensitivity: case studies from Atlanta, New York, and Los Angeles. J. Air Waste Manag. Assoc. 47, 642–652.
Stajner, I., Davidson, P., Byun, D., McQueen, J., Draxler, R., Dickerson, P., Meagher, J., 2011. US National Air Quality Forecast Capability: Expanding Coverage to Include Particulate Matter. Springer, Dordrecht, pp. 379–384. https://doi.org/10.1007/978-94-007-1359-8_64.
Tang, Y., et al., 2009. The impact of lateral boundary conditions on CMAQ predictions over the continental United States. Environ. Fluid Mech. 9, 43–58. https://doi.org/10.1007/s10652-008-9092-5.
Tong, D.Q., Lee, P., Saylor, R.D., 2012. New Direction: the need to develop process-based emission forecasting models. Atmos. Environ. 47, 560–561.
Tong, D.Q., Lamsal, L., Pan, L., Ding, C., Kim, H., Lee, P., Chai, T., Pickering, K.E., Stajner, I., 2015. Long-term NOx trends over large cities in the United States during the 2008 Recession: intercomparison of satellite retrievals, ground observations, and emission inventories. Atmos. Environ. 107, 70–84. https://doi.org/10.1016/j.atmosenv.2015.01.035.
Tong, D., Pan, L., Chen, W., Lamsal, L., Lee, P., Tang, Y., Kim, H., Kondragunta, S., Stajner, I., 2016. Impact of the 2008 Global Recession on Air Quality over the.
U.S. Energy Information Administration (EIA), 2020 Aug 11. Short-Term Energy Outlook [cited August 18, 2020]. Available from: https://www.eia.gov/outlooks/steo/.
U.S. EPA, 2012. Office of Research and Development. In: 2012, February 29). CMAQv5.0 (Version 5.0). https://doi.org/10.5281/zenodo.1079888. Zenodo.
U.S. EPA, 2015. Office of Air Quality Planning and Standards. 2011 National Emissions Inventory version 2. Technical Support Document (August 2015). Available from: https://www.epa.gov/sites/production/files/2015-10/documents/nei2011v2_tsd_14aug2015.pdf.
U.S EPA, 2018. Office of Air Quality Planning and Standards. 2014 National Emissions Inventory version 2. Technical Support Document (July 2018). Available from: https://www.epa.gov/sites/production/files/2018-07/documents/nei2014v2_tsd_05jul2018.pdf.
U.S. EPA, 2020. Nonattainment Areas for Criteria Pollutants (Green Book). July 31, 2020. Available from: https://www.epa.gov/green-book.
U.S. News, 2020. Low U.S. Traffic Levels 'Unprecedented' amid Coronavirus. 2020 Apr 15 [cited August 18, 2020]. Available from: https://www.usnews.com/news/best-states/articles/2020-04-15/low-us-traffic-levels-unprecedented-during-coronavirus-pandemic.
Van Haasen, N., 2020. Effects of COVID-19 on transportation and air quality in the north central Texas region. In: CMAS Virtual Conference, 2020. October 26-30, 2020.
Venter, Z. S. Venter, Aunan, Kristin, Chowdhury, Sourangsu, Lelieveld, Jos, 2020. COVID-19 lockdowns cause global air pollution declines. Aug 2020 Proc. Natl. Acad. Sci. Unit. States Am. 117 (32), 18984–18990. https://doi.org/10.1073/pnas.2006853117.
Wałaszek, K., Kryza, M., Werner, M., 2018. The role of precursor emissions on ground level ozone concentration during summer season in Poland. J. Atmos. Chem. 75, 181–204. https://doi.org/10.1007/s10874-017-9371-y, 2018.
Wu, X., Nethery, R.C., Sabath, M.B., Braun, D., Dominici, F., Air pollution and COVID-19 mortality in the United States, 2020. Strengths and limitations of an ecological regression analysis. Sci. Adv. 6, eabd4049.
Yang, J., Wang, Y., Henderson, B., Pinto, J., 2020. Improvement of the air quality in the LA basin during the COVID 19 outbreak based on real time data and CMAQ. In: CMAS Virtual Conference, 2020. October 26-30, 2020.
Yue, X., Lei, Y.D., Zhou, H., Liu, Z., Cai, Z., Lin, J., Jiang, Z., Liao, H., 2020. Changes of anthropogenic carbon emissions and air pollutants during the COVID-19 epidemic in China (in Chinese). Trans. Atmos. Sci. 43, 265–274.
Zhang, J. Y. Wei, Fang, Z., 2019. Ozone pollution: a major health hazard worldwide. Front. Immunol. 10, 2518. https://doi.org/10.3389/fimmu.2019.02518.
Zhang, Y., Wen, X.-Y., Wang, K., Vijayaraghavan, K., Jacobson, M.Z., 2009. Probing into regional ozone and particulate matter pollution in the United States: 2. An examination of formation mechanisms through a process analysis technique and sensitivity study. J. Geophys. Res. 114.
Zhang, R., Zhang, Y., Lin, H., Feng, X., Fu, T.-M., Wang, Y., 2020. NOx emission reduction and recovery during COVID-19 in east China. Atmosphere 11, 433.

Further reading

United States: Implications for surface ozone levels from changes in NOx emissions, Geophys. Res. Lett., 43, 9280–9288, doi:10.1002/2016GL069885.